Nonlinear Dynamics of Twisted and Coiled Polymer Actuator made of Conductive Nylon based on the Energy Balance

Ken Masuya[1], Shu Ono[1], Kentaro Takagi[2] and Kenji Tahara[1]

***Abstract*— This paper proposes a novel dynamics model of the twisted and coiled polymer actuator (TCPA) which is one of the artificial muscles recently discovered. It can be driven by Joule heating and can contract up to 25%. Most of the conventional works employed the linear model of TCPA which represents the relationships between the input voltage, the temperature, and the displacement, but the real TCPA shows the nonlinearity. Although a nonlinear model was proposed based on the curve fitting, it is difficult to apply the model to the various TCPAs. Additionally, the conventional works cannot explain the effect of the convective heat transfer condition on the displacement behavior of TCPA. This paper aims to construct a general nonlinear model of TCPA based on the following two ideas: (1) The energy balance of TCPA and (2) the temperature and velocity dependence of the heat transfer coefficient. The temperature model is obtained from the time derivative of the energy balance, and the displacement model is derived as Lagrange's equation of motion with the dissipation function. Through experiments, it is verified that the proposed model is closer to the real dynamics than the conventional linear model.**

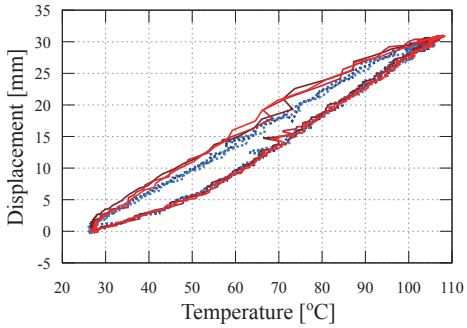

Fig. 1. Relationship between the temperature and the displacement of a TCPA. The solid lines with red tone and the dotted lines with blue tone represent the case with and without the fan when cooling, respectively. TCPA was fabricated by twisting three conductive nylon (AGposs 100/34 2ply, Mitsufuji) in the same time. We input the step voltage to TCPA and conducted three trials in each case. It is verified that the path is varied with the difference of the convective heat transfer.

I. INTRODUCTION

It is expected to apply the robotics to the welfare field such as the rehabilitation, the prosthesis, and the motion assistance. Actuators for them are required to be soft in order not to injure humans when the contact occurs, while those are necessary to be powerful to support their motion. The twisted and coiled polymer actuator (TCPA [1], [2], [3]), which is also known as the fishing line artificial muscle [4], [5], the coiled fishing line actuator [6], the super-coiled polymer actuator [7], the nylon actuator [8] and so on, is one option of such actuator. TCPA is fabricated by twisting polymer fibers such as nylon and polyethylene, and contracts by heating [4]. Its stroke is up to 25 %, and its specific power runs up to 5.26 kW/kg, which is over 100 times as large as that of human muscle. Additionally, there is less hysteresis than the shape-memory-alloy (SMA) which is driven by heating as well as TCPA.

The methods to heat TCPA are roughly divided into two methods. One method is to expose TCPA to hot water [4], [6]. Although the heat can be rapidly exchanged by using the water, it requires some external equipment such as the pump, the water reservoir, and the heater for the water. The other is based on Joule heating occurred on the resistance [1], [2], [3], [4], [5], [7], [8]. It can be easily controlled by the input voltage, so that we considers this method hereafter.

Several models of TCPA driven by Joule heating were proposed in the field of robotics and used to design the controller of TCPA. Yip and Niemeyer [7] modeled the relationship between the input voltage and the temperature of TCPA as a first-order linear transfer function and that between the temperature and the displacement as a second-order linear transfer function. Arakawa et al. [5] and Sutton et al. [8] employed the similar idea. However, in their temperature model, the input energy due to Joule heating is only used for the convective heat transfer and the temperature change despite the existence of the mechanical work. Additionally, the nonlinearity of the relationship between the displacement and the temperature of TCPA is verified by Haines et al. [4]. Based on the curve fitting, Cho et al. [3] identified a nonlinear displacement model. Although the simulation result by their model was close to the experimental result, it is difficult to apply the model to other TCPA. Furthermore, conventional models of TCPA cannot theoretically explain the phenomenon that the difference of the convective heat transfer condition affects the behavior of TCPA as shown in Fig. 1.

This paper aims to construct a nonlinear dynamics model of TCPA which can be applied to various TCPAs and take the effect of the convective heat transfer on the displacement into consideration. The proposed model is obtained based on the following two ideas. The first idea is the energy balance

[1]Ken Masuya, Shu Ono, and Kenji Tahara are with the Department of Mechanical Engineering, Faculty of Engineering, Kyushu University, 744 Motooka, Nishi-ku, Fukuoka, Japan masuya@mech.kyushu-u.ac.jp

[2]Kentaro Takagi is with the Sub-department of Mechatronics, Department of Mechanical Science and Engineering, Graduate School of Engineering, Nagoya University, Furo-cho, Chikusa-ku, Nagoya, Japan takagi@nuem.nagoya-u.ac.jp

which is used for modeling the behavior of SMA [9], [10]. The nonlinear model of the temperature is derived from this idea. The second idea is the temperature and velocity dependence of the heat transfer coefficient. From this idea, the effect of the convective heat transfer on the displacement can be derived theoretically.

II. RELATED WORKS

A. Temperature model

Yip and Niemeyer [7] proposed the following temperature model based on Newton's law of cooling.

$$C_v\dot{T} = \frac{V_{\rm in}^2}{R} - \alpha S_c \Delta T, \tag{1}$$

$$\Delta T \equiv T - T_{\rm env} \tag{2}$$

where T is the temperature of TCPA, $T_{\rm env}$ is the ambient temperature. In the implementation, the representative temperature measured by sensors such as the thermistor [3], the infrared temperature sensor [5], and the thermocouple [7] is used as T. C_v is the heat capacity of TCPA, α is the heat transfer coefficient between TCPA and the fluid, S_c is the area of the surface exposed to the fluid, $V_{\rm in}$ is the input voltage, and R is the resistance of the heater. The first and second term on the right side of Eq. (1) mean Joule heating and the convective heat transfer, respectively.

By integrating Eq. (1) by the time, we can get the energy balance represented as

$$E_T = E_{\rm in} - E_{\rm conv}, \tag{3}$$

where E_T, $E_{\rm in}$, and $E_{\rm conv}$ denote the internal energy of TCPA, the energy input to TCPA, and the energy released from TCPA to the environment by the convective heat transfer, respectively, and are written as

$$E_T = \int C_v\dot{T}{\rm d}t, \tag{4}$$

$$E_{\rm in} = \int \frac{V_{\rm in}^2}{R}{\rm d}t, \tag{5}$$

$$E_{\rm conv} = \int \alpha S_c \Delta T {\rm d}t. \tag{6}$$

Eq. (3) means the input energy $E_{\rm in}$ is only used in E_T and $E_{\rm conv}$. However, some parts of the input energy are transduced into the mechanical energy of TCPA and the energy released from TCPA to the environment by the radiative heat transfer. Additionally, from the viewpoint of the thermal engineering, α depends on the temperature [9], [11] and velocity of TCPA (see Appendix A).

B. Displacement model

Yip and Niemeyer [7] proposed the linear model of the displacement based on the experimental result as follows.

$$m\ddot{x} + b\dot{x} + k_s x = c\Delta T, \tag{7}$$

where m, b, and k_s are the mass, the damping, and the spring stiffness of TCPA, respectively. x is the displacement of TCPA from the stationary position when the weight is hanged and $T = T_{\rm env}$. c is the temperature coefficient to add the temperature effect on the displacement. Based on the similar idea, Arakawa et al. [5] and Sutton et al. [8] represented the displacement model as the linear transfer function. However, the real behavior of TCPA is nonlinear [4]. Although Cho et al. [3] identified a nonlinear model from the experimental data based on the curve fitting, it is difficult to apply their model to other TCPA. Additionally, those models cannot theoretically explain the effect of the heat convective transfer as shown in Fig. 1.

III. NONLINEAR MODEL OF TCPA BASED ON ENERGY RELATED TO TCPA

A. Energy related to TCPA

Our goal is to construct a general nonlinear model of TCPA which can explain the effect of the convective heat transfer. For this purpose, we first focus on energies of TCPA.

In addition to E_T, $E_{\rm in}$, and $E_{\rm conv}$, let us consider the following four energy: namely, the mechanical kinetic energy E_K, the potential energy E_P, the dissipation energy due to the damping E_b, and the energy released from TCPA to the environment by the radiative heat transfer $E_{\rm emi}$. They are written as

$$E_K = \frac{1}{2}m\dot{x}^2, \tag{8}$$

$$E_P = \frac{1}{2}k_s x^2, \tag{9}$$

$$E_b = \int \frac{1}{2}b\dot{x}^2 {\rm d}t, \tag{10}$$

$$E_{\rm emi} = \int S_{\rm emi}\epsilon\sigma\left(T^4 - T_{\rm env}^4\right){\rm d}t, \tag{11}$$

where $S_{\rm emi}$ is the area of the surface which the heat radiates from, ϵ is the emissivity of TCPA, and σ is Stefan-Boltzmann constant.

B. Nonlinear model of the displacement

Assume that the generalized coordinate is the displacement, Lagrangian of TCPA is defined as

$$L \equiv E_K - E_P. \tag{12}$$

Additionally, we regard the rest of energies as the dissipation function. Therefore, Lagrange's equation of motion is represented as

$$\frac{\rm d}{{\rm d}t}\left(\frac{\partial L}{\partial \dot{x}}\right) = \frac{\partial L}{\partial x} - \frac{\partial \dot{E}_D}{\partial \dot{x}}, \tag{13}$$

where E_D is the dissipation function and is written as

$$E_D = E_T + E_b + E_{\rm conv} + E_{\rm emi} - E_{\rm in}. \tag{14}$$

Focus on the dissipation function, $E_{\rm conv}$ can be expressed as the function of the velocity of TCPA $\dot{x}$ (see Appendix A) in addition to E_b. Thus, the second term of the right-hand side of Eq. (13) is represented as

$$\frac{\partial E_D}{\partial \dot{x}} = b\dot{x} + \frac{\partial \alpha(\dot{x}, T)}{\partial \dot{x}} S_c \Delta T. \tag{15}$$

In the modeling of SMA, α is approximated by the quadratic function [11] and the polynomial [9]. In order to take the

Fig. 2. The machine to fabricate TCPA. TCPA is fabricated by twisting DC motor attached on the upper end of the nylon thread.

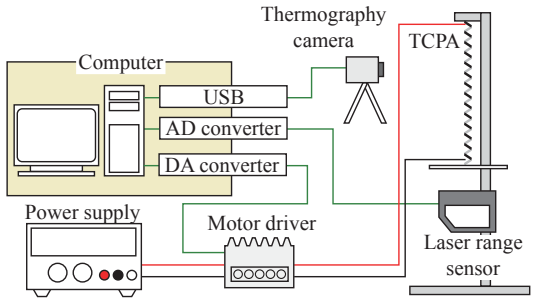

Fig. 3. The overview of the experimental environment

nonlinearity into consideration, this paper approximates α as the quadratic function of $\dot{x}$ and T by Taylor expansion around $\dot{x} = 0$ and $\Delta T = 0$, namely,

$$\alpha(\dot{x}, T) \simeq \alpha_0 + \alpha_x \dot{x} + \alpha_T \Delta T + \frac{1}{2}\alpha_{xx}\dot{x}^2 + \alpha_{xT}\dot{x}\Delta T + \frac{1}{2}\alpha_{TT}\Delta T^2, \quad (16)$$

By Eqs. (13), (15), and (16), the nonlinear model of TCPA's displacement is derived as

$$m\ddot{x} + (b + \alpha_{xx} S_c \Delta T)\dot{x} + k_s x = \alpha_x S_c \Delta T + \alpha_{xT} S_c \Delta T^2 \quad (17)$$

where we set the positive direction of x to the contraction direction of TCPA. Obviously, Eq. (17) includes Eq. (7), and can explain the effect of the heat transfer coefficient.

C. Nonlinear model of the temperature

As well as the model of SMA [9], [10], the energy balance of TCPA is written as

$$E_T + E_K + E_P + E_b + E_{\mathrm{conv}} + E_{\mathrm{emi}} = E_{\mathrm{in}}. \quad (18)$$

Thus, the nonlinear model of the temperature is obtained by differentiating Eq. (18) by the time, and is represented as

$$C_v \frac{\mathrm{d}T}{\mathrm{d}t} = \frac{V_{\mathrm{in}}^2}{R} - \alpha S_c \Delta T - S_{\mathrm{emi}}\epsilon\sigma\left(T^4 - T_{\mathrm{env}}^4\right) - m\dot{x}\ddot{x} - \frac{1}{2}b\dot{x}^2 - k_s x\dot{x}. \quad (19)$$

By Eqs. (16) and (17), the temperature model is rewritten as

$$C_v \frac{\mathrm{d}T}{\mathrm{d}t} = \frac{V_{\mathrm{in}}^2}{R} - \alpha_0 S_c \Delta T - \alpha_T S_c \Delta T^2 - \alpha_{TT} S_c \Delta T^3 + \frac{1}{2}\alpha_{xx}\dot{x}^2 S_c \Delta T + \frac{1}{2}b\dot{x}^2 - S_{\mathrm{emi}}\epsilon\sigma\left(T^4 - T_{\mathrm{env}}^4\right). \quad (20)$$

As well as the displacement model, Eq. (20) includes Eq. (1).

IV. EVALUATION THROUGH EXPERIMENTS

A. Fabrication of TCPA

In order to evaluate the validity of the proposed nonlinear model in the various TCPAs, two TCPAs were used in the experiment. One was fabricated by overtwisting three conductive nylon AG-poss 100/34 2ply (Mitsufuji) in the same time, based on the fabrication of Cho et al.[2]. The other was made of a conductive nylon PN#260151023534(235/34 4ply, Shieldex). Hereafter, TCPA made of nylon produced by Mitsufuji and Shiledex are called "Mitsufuji" and "Shieldex," respectively. As shown in Fig. 2, we hanged the weight about 90g at one end in the fabrication, and another end was connected to the DC motor. Finally, both coiled nylons were heated up to 180 °C by the automatic oven (OFW-300B, AS ONE) for the thermal treatment.

B. Experimental environment

The overview of the experimental environment is shown in Fig. 3. The displacement of TCPA was measured by the laser range sensor (IL-300, KEYENCE) and the measurement was obtained through the amplifier (IL-1000, KEYENCE) and the AD converter (AD16-16U(PCI)EV, CONTEC). On the other hand, the temperature of TCPA was measured by the thermography camera (OPTPI230O23T900, Optris). TCPA was driven by the voltage produced by the motor driver (LSC 30/2, Maxon motor) which the reference was given to by the analog output from the DA converter (PCI-3340, Interface). The sampling frequency was set to 100Hz. In the following experiments, we hanged the weight about 55g and 101g at one end of Mitsufuji and Shieldex, respectively.

C. Identification

First, we independently identified parameters in Eqs. (17) and (20) by the nonlinear least square method.

We selected the following step voltage as the input to TCPA to identify both the temperature and displacement model.

$$V_{\mathrm{in}}(t) = \begin{cases} \sqrt{V_{\mathrm{ref}}^2} & (10 \le t < 70) \\ 0 & (0 \le t < 10, 70 \le t < 150) \end{cases}, \quad (21)$$

where V_{ref} is the reference voltage. The maximum value of V_{ref} was determined so as that the maximum temperature exceeds 110 °C. In the experiment, V_{ref}^2 of Mitsufuji was set to 20, 40, and 60, and that of Shieldex was set to 40, 80, and 120. For each voltage, we collected five data.

TABLE I

IDENTIFIED PARAMETERS OF THE TEMPERATURE MODEL. (W. : WITH, WO. : WITHOUT)

TCPA	Model	$\alpha(\dot{x},T)$	E_{emi}	E_b	$\frac{1}{RC_v}$	$\frac{\alpha_0 S_c}{C_v}$	$\frac{\alpha_T S_c}{C_v}$	$\frac{\alpha_{TT} S_c}{C_v}$	$\frac{\alpha_{xx} S_c}{C_v}$	$\frac{S_{\mathrm{emi}}}{C_v}$	$\frac{b}{C_v}$	Fitness
					$\times 10^{-1}$ [K/(J·Ω)]	$\times 10^{-1}$ [1/s]	$\times 10^{-4}$ [1/(K·s)]	$\times 10^{-6}$ [1/(K^2·s)]	$\times 10$ [s/m^2]	$\times 10^{-2}$ [m^2·K/J]	$\times 10^{2}$ [K·s/m^2]	[%]
Mitsufuji	Yip&Niemeyer	wo.	wo.	wo.	2.234	1.546						99.63
	E_b	wo.	wo.	w.	2.234	1.546					1.076	99.63
	E_{emi}	wo.	w.	wo.	2.425	1.704				0.013		99.55
	$E_b + E_{\mathrm{emi}}$	wo.	w.	w.	2.440	1.723				0.002	1.987	99.56
	$\alpha(\dot{x},T)$	w.	wo.	wo.	2.275	1.706	0.866	-3.455	-0.657			99.91
	$\alpha(\dot{x},T) + E_b$	w.	wo.	w.	2.275	1.709	0.794	-3.409	-1.524		4.816	99.91
	$\alpha(\dot{x},T) + E_{\mathrm{emi}}$	w.	w.	wo.	2.275	1.687	0.757	-3.470	-0.657	0.032		99.91
	Proposed	w.	w.	w.	2.275	1.709	0.793	-3.409	-1.524	0.000	4.816	99.91
Shieldex	Yip&Niemeyer	wo.	wo.	wo.	1.143	1.496						99.64
	E_b	wo.	wo.	w.	1.143	1.496					0.040	99.64
	E_{emi}	wo.	w.	wo.	1.144	1.309				0.223		99.66
	$E_b + E_{\mathrm{emi}}$	wo.	w.	w.	1.144	1.309				0.223	0.204	99.66
	$\alpha(\dot{x},T)$	w.	wo.	wo.	1.146	1.282	6.289	-4.208	-0.483			99.67
	$\alpha(\dot{x},T) + E_b$	w.	wo.	w.	1.146	1.282	6.288	-4.207	-0.500		0.084	99.67
	$\alpha(\dot{x},T) + E_{\mathrm{emi}}$	w.	w.	wo.	1.146	0.000	0.565	-6.513	-0.477	2.158		99.67
	Proposed	w.	w.	w.	1.146	0.000	0.565	-6.513	-0.477	2.158	0.000	99.67

TABLE II

IDENTIFIED PARAMETERS OF THE DISPLACEMENT MODEL (W. : WITH, WO. : WITHOUT)

TCPA	Model	Temperature dependent damper	Quadratic Term of Temperature	$\frac{b}{m}$	$\frac{k_s}{m}$	$\frac{\alpha_x S_c}{m}$	$\frac{\alpha_{xT} S_c}{m}$	$\frac{\alpha_{xx} S_c}{m}$	f_1	f_2	Fitness
				$\times 10^{2}$ [1/s]	$\times 10^{2}$ [1/s^2]	$\times 10^{-1}$ [m/(s^2·K)]	$\times 10^{-4}$ [m/(s^2·K^2)]	$\times 10^{-2}$ [1/(K·s)]	[Hz]	[Hz]	[%]
Mitsufuji	Yip&Niemeyer	wo.	wo.	5.067	1.028	0.376			0.032	80.62	94.46
	TDD	w.	wo.	5.194	3.249	0.986		-0.750	0.104	88.65	98.86
	QT	wo.	w.	5.577	3.645	1.081	3.452		0.100	82.56	99.02
	Proposed	w.	w.	5.287	2.015	0.534	8.014	1.411	0.060	84.08	98.82
Shieldex	Yip&Niemeyer	wo.	wo.	5.433	0.752	0.192			0.022	86.45	91.51
	TDD	w.	wo.	6.162	5.157	0.965		-1.828	0.100	98.15	99.39
	QT	wo.	w.	6.173	3.891	0.685	4.182		0.133	97.94	99.38
	Proposed	w.	w.	5.634	3.242	0.640	-2.248	-1.845	0.092	89.58	99.05

Identification results are tabulated in Tables I and II. f_1 and f_2 in Table II are the natural frequency of Eq. (17) at $\Delta T = 0$, and are computed as

$$f_1, f_2 = \frac{b}{4\pi m} \pm \frac{1}{4\pi}\sqrt{\left(\frac{b}{m}\right)^2 - 4\frac{k_s}{m}}, \quad f_1 \le f_2.$$

E_{rad}, E_b, and $\alpha(\dot{x},T)$ in Table I mean the model including the radiation term, the damping term, and the temperature and velocity dependent heat transfer coefficient, respectively.

Table I shows that $\frac{1}{RC_v}$ of all model are similar in each TCPA. This indicates that the heat capacity and the resistance can be assumed to be constant. $\frac{\alpha_0 S_c}{C_v}$ of $\alpha(\dot{x},T) + E_{\mathrm{emi}}$ and Proposed of Shieldex are zero unlike other models. This is because the radiation term absorbs the term of $\frac{\alpha_0 S_c}{C_v}$ in the case of Shieldex. Conversely, the value of $\frac{S_{\mathrm{emi}}}{C_v}$ is small in the case of Mitsufuji since the term of $\frac{\alpha_0 S_c}{C_v}$ absorbs. The fitness of the model with $\alpha(\dot{x},T)$ is slightly better than that without $\alpha(\dot{x},T)$, so that the temperature and velocity dependence of the convective heat transfer affects the validity of the temperature model.

The fitness in Table II indicates that both the quadratic term of the temperature and the temperature dependent damper can improve the validity of the model, and the fitness of TDD is better than that of QT comprehensively. Due to the interference of those terms, the fitness of Proposed is slightly lower than TDD and QT. Focus on f_1 and f_2, f_2 is close to the sampling frequency. This is because m is negligibly small. This indicates that the displacement behavior can be approximated as the first-order model as Arakawa et al. [5] did. Additionally, it is verified that f_1 of Yip&Niemeyer is the lowest frequency compared with other models.

In the following experiments, we only compared the proposed model and Yip & Niemeyer [7] in the evaluation of both the temperature and displacement model.

D. Results of the step input

The input is the same as shown in Eq. (21). The same reference voltage was used in the experiment, and we re-collected five data for each voltage.

Figs. 4 and 5 shows the estimation results. RMSE(T) and RMSE(x) in Figs. 4 and 5 are the normalized root-mean-square error of the temperature and displacement, respectively. Those are represented as

$$\mathrm{RMSE}(T) = \sqrt{\frac{1}{N}\sum_{i=1}^{N}\frac{(\hat{T}-\tilde{T})^2}{\Delta T_{\max}}} \times 100, \tag{22}$$

$$\mathrm{RMSE}(x) = \sqrt{\frac{1}{N}\sum_{i=1}^{N}\frac{(\hat{x}-\tilde{x})^2}{x_{\max}}} \times 100, \tag{23}$$

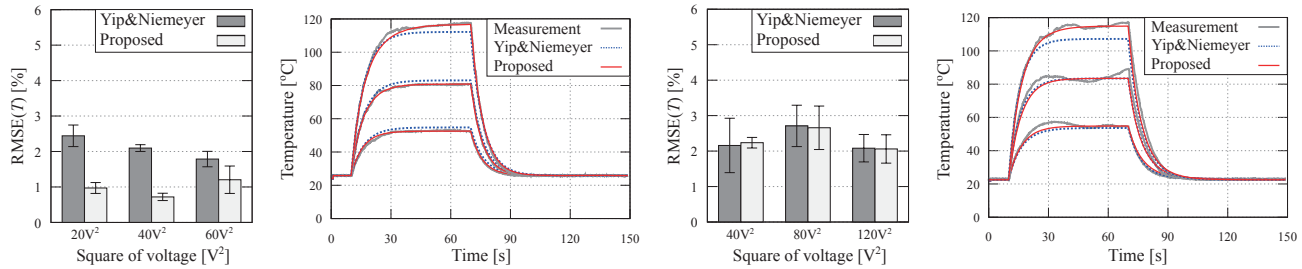

(a) The estimation error of Mitsufuji (b) The estimation result of Mitsufuji (c) The estimation error of Shieldex (d) The estimation result of Shieldex

Fig. 4. The estimation results of the temperature in the case of the step input. (Error bar means the standard deviation.)

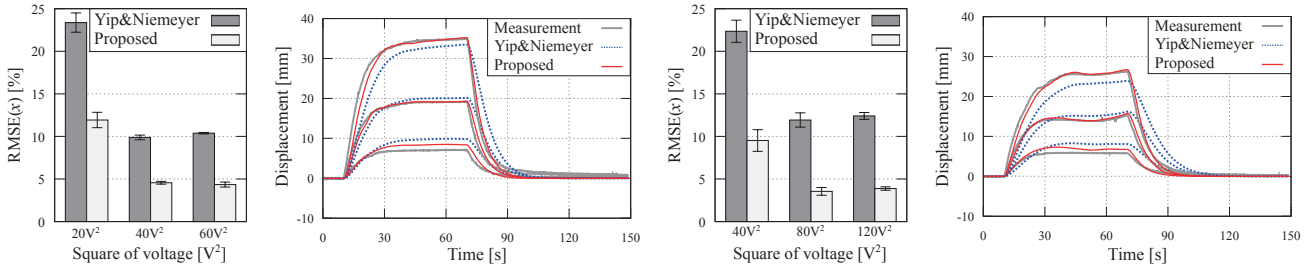

(a) The estimation error of Mitsufuji (b) The estimation result of Mitsufuji (c) The estimation error of Shieldex (d) The estimation result of Shieldex

Fig. 5. The estimation results of the displacement in the case of the step input. (Error bar means the standard deviation.)

where $\Delta T_{\max}$ and $x_{\max}$ are the maximum value of ΔT and x, respectively. $\hat{*}$ and $\tilde{*}$ mean the estimated and measured value of $*$, respectively.

RMSE(T) in Figs. 4(a) and 4(c) are consistent with those in Table I, namely, the estimation accuracy of the proposed model is better than Yip&Niemeyer in the case of Mitsufuji and is nearly the same in the case of Shieldex. Fig. 4(b) shows that Yip&Niemeyer has the offset error in the result of Mitsufuji at the end-point temperature. On the other hand, the proposed model can reduce the offset due to the temperature and velocity dependence of the convective heat transfer.

The results in Figs. 5(a) and 5(c) is also consistent with those in Table II, namely, the proposed model can improve the validity of the model. Figs. 5(b) and 5(d) show that the proposed model can reduce the offset compared with Yip&Niemeyer, in particular, when the displacement is large. Additionally, it is verified that the displacement of the proposed model rapidly decreases when cooling. This is because f_1 of the proposed model is larger than that of Yip&Niemeyer.

E. Results of the sinusoidal-like input

The following voltage was input to TCPA to vary the power sinusoidally,

$$V_{\mathrm{in}}(t) = \sqrt{\frac{V_{\mathrm{ref,max}}^2}{2}\left(1 - \cos(0.04\pi t)\right)}. \tag{24}$$

In the experiment, $V_{\mathrm{ref,max}}^2$ of Mitsufuji and Shieldex are respectively set to 60 and 120, and we collected five data.

The estimation results of the temperature and displacement are shown in Figs. 6 and 7, respectively. As well as the result in Figs. 4(a) and 4(c), RMSE(T) of the proposed model is reduced in Mitsufuji and is nearly the same as Yip&Niemeyer in Shieldex. However, the absolute value of RMSE(T) of Mitsufuji increases. The possible cause is the temperature fluctuation shown in Fig. 6(b). On the other hand, the proposed displacement model can improve the estimation accuracy in both TCPAs. This is due to the reduction of the lag shown in Figs. 7(b) and 7(c).

V. CONCLUSION

This paper proposes a nonlinear model of TCPA's temperature and displacement. The proposed model is theoretically derived from the idea of the energy balance and the temperature and velocity dependent heat transfer coefficient. Additionally, the proposed model includes the conventional model. Through experiments, it is verified that the proposed model can reduce the estimation error compared with the conventional linear model, in particular, the displacement.

APPENDIX

A. Temperature and velocity dependence of the heat transfer coefficient α

Assumed that the actuation of TCPA causes the forced convection. By using Nusselt number Nu, the heat transfer coefficient α is represented as

$$\alpha = \frac{k}{\bar{l}}\mathrm{Nu}, \tag{25}$$

where $\bar{l}$ is the representative length and k is the thermal conductivity of the fluid. Nu can be expressed as the function

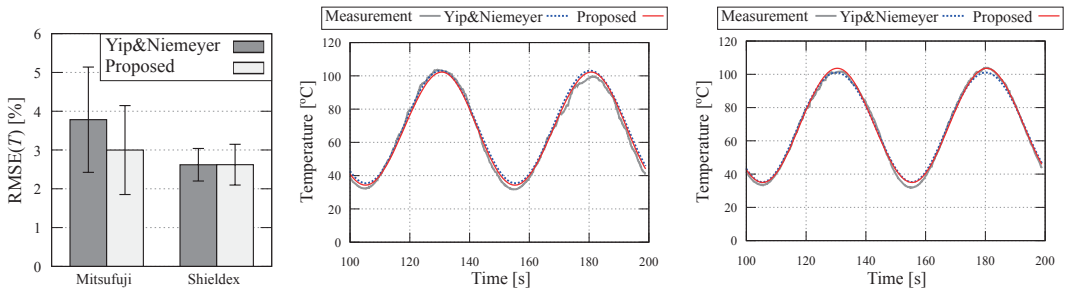

(a) The estimation error (b) The estimation result of Mitsufuji (c) The estimation result of Shieldex

Fig. 6. The estimation results of the temperature in the case of the sinusoidal-like input. (Error bar means the standard deviation.)

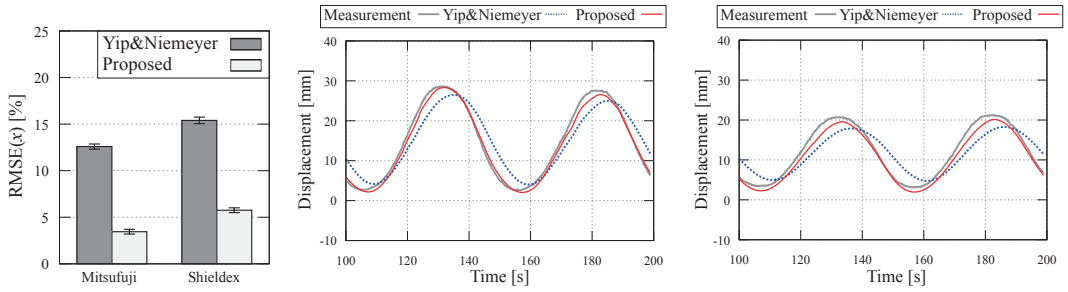

(a) The estimation error (b) The estimation result of Mitsufuji (c) The estimation result of Shieldex

Fig. 7. The estimation results of the displacement in the case of the sinusoidal-like input. (Error bar means the standard deviation.)

of other non-dimensional numbers as follows [12]:

$$\mathrm{Nu} = \mathrm{Nu}(\mathrm{Re}, \mathrm{Pr}) \tag{26}$$

where Re and Pr mean Reynolds number and Prandtl number, respectively. Those are represented as

$$\mathrm{Re} = \frac{v\bar{l}}{\nu}, \qquad \mathrm{Pr} = \frac{\nu}{\gamma},$$

where ν is the kinematic viscosity of the fluid, γ is the thermal diffusivity of the fluid, and v is the relative velocity between the fluid and TCPA.

Since Re is related to TCPA's velocity $\dot{x}$, Nusselt number can be expressed as the function of $\dot{x}$. Furthermore, ν depends on the temperature in general [12], so that we can regard Re and Pr as the function of TCPA's temperature T. Thus, Nusselt number Nu can be rewritten as

$$\mathrm{Nu} = \mathrm{Nu}(\dot{x}, T). \tag{27}$$

From Eqs. (25) and (27), α is also expressed as the function of the temperature and velocity of TCPA, namely,

$$\alpha = \alpha(\dot{x}, T). \tag{28}$$

ACKNOWLEDGMENT

This work was supported by "Research and development of Flexible Human Motion Support Device by using Polymeric Artificial Muscle Actuator" in Innovative Robotics Elemental Technology Field / Development of Next Generation Robotics Core Technology, the New Energy and Industrial Technology Development Organization (NEDO) and also partially supported by JSPS KAKENHI Grant Number JP17H03204.

REFERENCES

[1] L. Saharan and Y. Tadesse, "Robotic Hand with Locking Mechanism Using TCP Muscles for Applications in Prosthetic Hand and Humanoids," in Proc. of SPIE, vol. 9797, Las Vegas, NV, USA, Mar. 2016, 97970V.

[2] K. H. Cho et al., "A robotic finger driven by twisted and coiled polymer actuator," in Proc. of SPIE 9798, Las Vegas, NV, USA, Mar. 2016, 97981J.

[3] K. H. Cho et al, "Fabrication and Modeling of Temperature-controllable Artificial Muscle Actuator," in Proc. of the 6th IEEE RAS/EMBS Int. Conf. on Biomedical Robotics and Biomechatronics, UTown, Singapore, Jun. 2016, pp.94–98.

[4] C. S. Haines et al., "Artificial Muscles from Fishing Line and Sewing Thread," Science, vol. 343, no. 6173, pp. 868–872, Feb. 2014.

[5] T. Arakawa et al., "Position control of fishing line artificial muscles (coiled polymer actuators) from Nylon thread," in Proc. of SPIE, vol. 9798, Las Vegas, NV, USA, Mar. 2016, 97982W.

[6] L. Wu et al., "Nylon-Muscle-Actuated Robotic Finger," in Proc. of SPIE 9431, San Diego, CA, USA, Mar. 2015, 94310I.

[7] M. C. Yip and G. Niemeyer, "High-Performance Robotic Muscles from Conductive Nylon Sewing Thread," in Proc. of the 2015 IEEE Int. Conf. on Robotics and Automation, Seattle, WA, USA, May 2015, pp. 2313–2318.

[8] L. Sutton et al., "Design of an Assistive Wrist Orthosis Using Conductive Nylon Actuators", in Proc. of the 6th IEEE RAS/EMBS Int. Conf. on Biomedical Robotics and Biomechatronics, UTown, Singapore, Jun. 2016, pp.1074–1079.

[9] H. Meier and L. Oelschlaeger, "Numerical thermomechanical modelling of shape memory alloy wires," Materials Science and Engineering A, vol. 378, no. 1-2, pp. 484–489, Jul. 2004.

[10] F. Schiedeck and S. Mojrzisch, "Frequency-domain control design for shape memory alloy actuators," Sensors and Actuators A: Physical, vol. 169, no. 1, pp. 133–140, Sep. 2011.

[11] J. Jayender et al., "Modeling and Control of Shape Memory Alloy Actuators," IEEE Transaction on Control Systems Technology, vol. 16, no. 2, pp. 279–287, Mar. 2008.

[12] J. H. Lienhard, A heat transfer textbook. Englewood Cliffs, NJ: Prentice Hall, 1981.